Crystal structure of Na[N(SO_2CF_3)$_2$] and coordination environment of alkali metal cation in the M[N(SO_2CF_3)$_2$] (M^+ = Li^+, Na^+, K^+, and Cs^+) structures

Kazuhiko Matsumoto,* Toshifumi Matsui, Toshiyuki Nohira, Rika Hagiwara

Graduate School of Energy Science, Kyoto University, Sakyo-ku, Kyoto 606-8501, Japan,

*E-mail: k-matsumoto@energy.kyoto-u.ac.jp

Tel: +81-75-753-4817

Fax: +81-75-753-5906

Key words**:** TFSA, bis(trifluoromethylsulfonyl)amide, structure, alkali metal

Abstract

Crystal structure of Na[TFSA] ($TFSA^-$ = bis(trifluoromethylsulfonyl)amide anion ($N(SO_2CF_3)_2^-$)) has been determined by single-crystal X-ray diffraction. This compound crystallizes in a monoclinic cell (space group: $P2_1/n$) with Z = 8 and two ion pairs in the asymmetric unit. Both the crystallographically independent $TFSA^-$ anions adopt a *cis* configuration with the C−S···S−C torsion angle of −25.2(2)° and 25.1(2)°. The Na^+ cations have contacts primarily with five neighboring O atoms (2.344(3) − 2.415(3) Å for Na1···O and 2.337(3) − 2.451(3) Å for Na2···O) and secondarily with one O atom and one N atom (2.843(3) for Na1···O, 2.929(3) for Na1···N, 2.806(3) for Na2···O and 2.907(3) for Na2···N). Comparison of the present structure with the previously reported M[TFSA] (M^+ = Li^+, K^+, and Cs^+) structures revealed that all of them have layered structures composed of the cationic and anionic layers. Coordination environment of M^+ in the M[TFSA] structures is discussed based on bond valence sum calculations.

1. Introduction

The bis(trifluoromethylsulfonyl)amide (TFSA) group was first introduced as a compound Xe[TFSA]$_2$ [1, 2], followed by a number of TFSA$^-$ salts including M[TFSA] ($M^+ = Li^+$, Na^+, K^+, Rb^+, and Cs^+) and organic salts [3-13]. The Li[TFSA] salt was intensively investigated as a solute of polymer electrolytes to improve safety issues of Li ion batteries [14]. Organic TFSA$^-$ salts such as 1-ethyl-3-methylimidazolium bis(trifluoromethylsufonyl)amide ([C_2C_1im][TFSA]) are now widely used as ionic liquids for synthetic and electrochemical works [11, 12, 15, 16]. The organic TFSA$^-$ salts generally have a number of preferable properties such as high hydrophobicity, low melting points, high decomposition temperatures, low viscosities, and high ionic conductivities. For example, [C_2C_1im][TFSA] exhibits a melting point of 257 K [17], an ionic conductivity of 8.8 mS cm^{-1} at 298 K [11], a viscosity of 34 mPa s at 298 K [11], and decomposition temperature around 690 K [17]. Application of M[TFSA] ionic liquids as electrolytes in lithium and sodium secondary batteries in an intermediate temperature range has been recently studied [18-20]. The robust structure of TFSA$^-$ enables the operation of these batteries even above 473 K. Furthermore, the TFSA-based plastic crystals also attract attention as highly conductive solid-state electrolytes [21, 22].

Understanding of structural features is important to design suitable electrolytes in specific applications such as secondary batteries. Crystal structures of Li[TFSA], K[TFSA], and Cs[TFSA] were determined by X-ray diffraction [3, 5, 6], whereas the structures of Na[TFSA] and Rb[TFSA] have not been reported. The anhydrous M[TFSA] ($M^+ = Li^+$, K^+, and Cs^+) structures are characterized by their layered structures dominated by intermolecular $M^+\cdots O$ (or N) interactions. The monohydrate of Li[TFSA], Li[TFSA]·H_2O, has a layered structure where Li^+ cation and H_2O molecule are located in the polar layer and Li^+ is octahedrally coordinated by six O atoms [3]. In the water and methanol solvate of Na[TFSA], Na[TFSA]·H_2O·CH_3OH, a layer of Na^+ and H_2O and another layer of TFSA$^-$ and CH_3OH alternate along the crystallographic *b* axis and the Na^+ has contacts with six oxygen atoms in an octahedral manner [3]. In these structures, the sulfonyl oxygen atoms in TFSA$^-$ predominantly interact with the cations while the bridging N atom only weakly does in some cases.

According to computational works on TFSA$^-$, the *trans*-conformer is more stable than the *cis*-conformer in gas phase [3, 23, 24], where *cis* and *trans* indicate the relative positions of the two CF_3 groups, i.e., on the same side or opposite sides, respectively, relative to the plane defined by the S−N−S bonds. Indeed the *trans*-conformer is experimentally found to be a dominant species in the liquid state [23], but the *cis*-conformer is observed in many crystal structures [3, 4]. The small energetic barrier between the two conformers sometimes leads to the *cis*-conformer in the solid state due to crystal packing effects.

In the present study, the crystal structure of Na[TFSA] determined by single-crystal X-ray diffraction is reported and is discussed in comparison with the previously known M[TFSA] structures. Coordination environment around M$^+$ in the series of the M[TFSA] structures is especially investigated in details based on bond valence sum calculations.

2. Results and discussion

2.1 Crystal structure of Na[TFSA]

Crystal data and refinement results for Na[TFSA] are given in Table 1. Important geometrical parameters are listed in Table 2. This compound crystallizes into the monoclinic space group $P2_1/c$. The ORTEP diagram of the asymmetric unit is shown in Fig. 1. The asymmetric unit is composed of two ion pairs, where TFSA$^-$ adopts a *cis*-conformation with the C−S···S−C torsion angle of −25.2(2)° for C1−S1···S2−C2 and 25.1(2)° for C3−S3···S4−C4. The intramolecular geometries of TFSA$^-$ are in good agreement with those in previously determined M[TFSA] (M+ = Li$^+$, K$^+$, and Cs$^+$) crystal structures (e.g., bond length range: N−S, 1.573(3)−1.579(3) Å; S−C, 1.842(4)−1.849(4) Å; S−O, 1.429(3)−1.446(3) Å; and C−F, 1.313(4)−1.327(4) Å and bond angle range: S−N−S, 126.6(2)° for both, N−S−C, 101.92(17)−106.00(17)°; N−S−O, 107.25(17)−117.47(17)°; O−S−O, 117.61(17)−117.92(17)°; S−C−F, 108.5(3)−110.5(3)°; and F−C−F, 108.9(3)−109.6(3)°) [3, 4].

Table 1 Crystal data and refinement results for Na[TFSA]

Formula	$Na_1N_1S_2O_4C_2F_6$
Formula weight	303.14
Temperature / K	100
Crystal system	Monoclinic
Space group	$P2_1/n$
a / Å	7.5696(3)
b / Å	10.4188(5)
c / Å	21.8468(10)
b / °	91.139(2)
V / Å^3	1722.63(13)
Z	8
Radiation	Mo $K\alpha$ (0.71073 Å)
d_c / g cm^{-3}	2.338
μ / mm^{-1}	0.772
R_1 $(I > 2\sigma(I))^a$	0.0502
$wR2$ $(I > 2\sigma(I))^b$	0.1287

$^bR_1 = \Sigma||F_o| - |F_c||/\Sigma|F_o|$. $^c\, wR_2 = [\Sigma w(F_o^2 - F_c^2)^2/\Sigma w(F_o^2)^2]^{1/2}$.

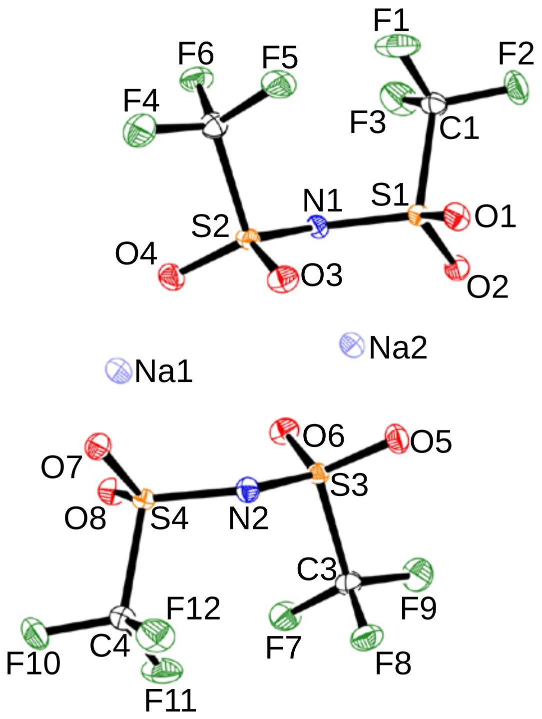

Fig. 1 ORTEP diagram of the asymmetric unit of Na[TFSA]. Thermal ellipsoids are shown at the 50% probability level.

Table 2 Experimental bond lengths (Å) and bond angles (°) for TFSA$^-$ in Na[TFSA]

N1−S1	1.573(3)	N1−S2	1.579(3)	N2−S3	1.575(3)
N2−S4	1.579(3)	S1−O1	1.429(3)	S1−O2	1.446(3)
S2−O3	1.444(3)	S2−O4	1.436(3)	S3−O5	1.431(3)
S3−O6	1.436(3)	S4−O7	1.445(3)	S4−O8	1.434(3)
S1−C1	1.842(4)	S2−C2	1.843(4)	S3−C3	1.843(4)
S4−C4	1.849(4)	C1−F1	1.318(5)	C1−F2	1.317(4)
C1−F3	1.316(5)	C2−F4	1.319(5)	C2−F5	1.324(4)
C2−F6	1.327(4)	C3−F7	1.325(5)	C3−F8	1.321(5)
C3−F9	1.325(5)	C4−F10	1.313(4)	C4−F11	1.318(5)
C4−F12	1.320(5)				
N1−S1−C1	102.13(17)	N1−S2−C2	106.00(17)	N2−S3−C3	105.40(17)
N2−S4−C4	101.92(17)	N1−S1−O1	117.25(17)	N1−S1−O2	107.59(16)
N1−S2−O3	114.82(16)	N1−S2−O4	108.09(17)	N2−S3−O5	108.35(17)
N2−S3−O6	115.29(16)	N2−S4−O7	107.58(16)	N2−S4−O8	117.47(17)
O1−S1−O2	117.76(16)	O2−S1−C1	104.02(18)	C1−S1−O1	106.04(18)
O3−S2−O4	117.76(17)	O4−S2−C2	104.27(17)	C2−S2−O3	104.65(17)
O5−S3−O6	117.61(17)	O6−S3−C3	104.67(17)	C3−S3−O5	104.10(17)
O7−S4−O8	117.92(16)	O8−S4−C4	105.90(17)	C4−S4−O7	103.89(17)
S1−C1−F1	110.2(3)	S1−C1−F2	109.5.(3)	S1−C1−F3	109.9(3)
S2−C2−F4	108.5(3)	S2−C2−F5	109.7(2)	S2−C2−F6	110.4(3)
S3−C3−F7	110.1(2)	S3−C3−F8	110.5(3)	S3−C3−F9	108.9(3)
S4−C4−F10	109.2(2)	S4−C4−F11	110.0(3)	S4−C4−F12	109.6(3)
F1−C1−F2	109.1(3)	F2−C1−F3	108.9(3)	F3−C1−F1	109.2(3)
F4−C2−F5	109.6(3)	F5−C2−F6	109.5(3)	F6−C2−F4	109.5(3)
F7−C3−F8	108.9(3)	F8−C3−F9	109.3(3)	F9−C3−F7	109.1(3)
F10−C4−F11	109.8(3)	F11−C4−F12	109.1(3)	F12−C4−F10	109.1(3)
C1−S1···S2−C2	−25.2(2)	C3−S3···S4−C4	25.1(2)°		

Although there is no obvious positional disordering in this structure, the F atoms in the terminal CF_3 groups have larger displacement parameters than those of the other atoms, suggesting some rotational freedom of the CF_3 group around the S-C bond.

The crystal packing of Na[TFSA] is shown in Fig. 2. The packing mode is best described as a layered structure where the cationic and anionic layers stack along the crystallographic *c* axis. The cationic layer is sandwiched by the O atoms of the anionic layer because Na^+ and the O atoms in TFSA$^-$ interact with each other, which results in the fluorous layer of trifluoromethyl groups owing to the *cis*-conformation of TFSA$^-$. Consequently, the stacking pattern along the *c* axis is described as [(Na^+)–(S, C, O, and N atoms in TFSA$^-$)–(CF_3 groups in TFSA$^-$)–(CF_3 groups in TFSA$^-$)–(S, C, O, and N atoms in TFSA$^-$)]$_n$ and is quite similar to those observed in the K[TFSA], Cs[TFSA], and

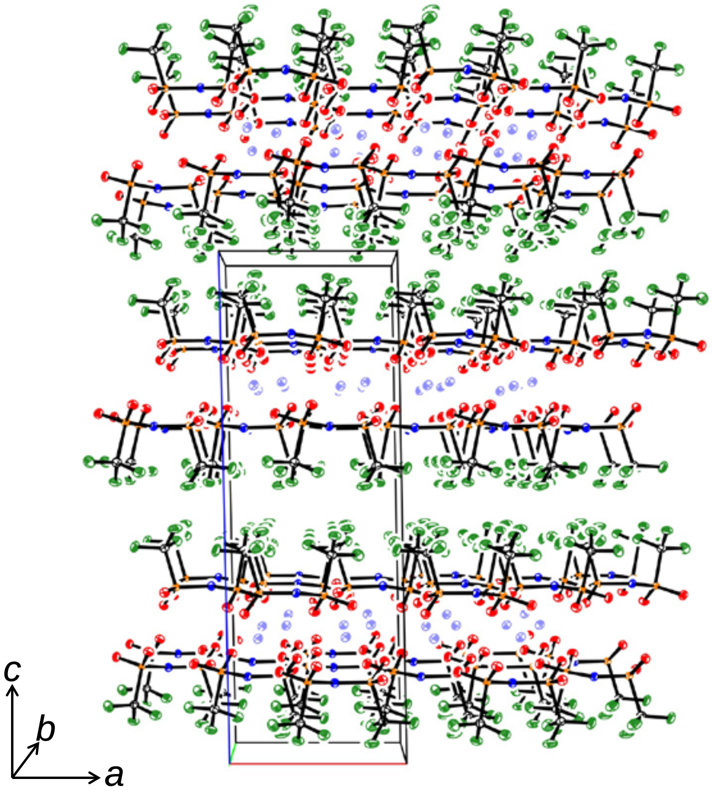

Fig. 2 Packing diagram of Na[TFSA] along the *b* axis. Thermal ellipsoids are shown at the 50% probability level.

Sr[TFSA]$_2$ structures [3, 4, 6]. Although the alternate cation and anion stacking is also observed in the Li[TFSA] structure, the *trans*-conformation of TFSA$^-$ leads to a simpler cation-anion stacking where TFSA$^-$ bridges Li$^+$ cations [5]. The repeating distance of the layered structure (*i.e.* the distance between the two nearest polar layers) is the half of the *c* cell parameter for the orthorhombic K[TFSA] structure and is calculated by multiplying the sinβ value by the half of the *c* cell parameter for the monoclinic Na[TFSA] (β = 91.139° and c = 21.8468 Å) or the *a* cell parameter for the monoclinic Cs[TFSA] (β = 92.12° and a = 22.428 Å) and the monoclinic Sr[TFSA] (β = 103.72(3)° and a = 11.199(4) Å). The repeating distances obtained are 10.9213, 11.173, 11.207, and 10.879 Å for Na[TFSA], K[TFSA], Cs[TFSA], and Sr[TFSA]$_2$, respectively. It should be noticed that the crystallographic repeating distance is twice as large as the values above except for the case of Sr[TFSA]$_2$. Although the slight differences in the repeating distances probably arise from the difference in the size of the cation, the four values are similar to each other, reflecting their structural similarity. The same stacking mode is also observed in the hydrates of Na[TFSA] (Na[TFSA]·H_2O) [3] and of alkali earth metal salts (Ca[TFSA]$_2$·4H_2O and Ba[TFSA]$_2$·H_2O) with *cis*-TFSA$^-$ [4]. Interestingly, all of the three hydrates have similar repeating distances (11.199, 11.190, and 11.157 Å for the monoclinic Na[TFSA]·H_2O, Ca[TFSA]$_2$·4H_2O, and Ba[TFSA]$_2$·H_2O structures, respectively) to those in Na[TFSA], K[TFSA], and Cs[TFSA], because the H_2O molecules located around the cations are included in the polar cationic layers and do not significantly affect the repeating distance.

2.2 Comparison of the coordination environment around M$^+$ in M[TFSA] (M$^+$ = Li$^+$, Na$^+$, K$^+$, and Cs$^+$)

Coordination environment around Na$^+$ in Na[TFSA] is shown in Fig. 3. The two crystallographically independent Na$^+$ (Na1 and Na2) cations have similar coordination environments. The Na$^+$ cation has primary contacts with five O atoms (Na1···O8, 2.344(3) Å; Na1···O4, 2.346(3) Å, Na1···O2, 2.395(3) Å; Na1···O7, 2.411(3) Å; Na1···O3, 2.415(3) Å; Na2···O1, 2.337(3) Å; Na2···O5, 2.385(3) Å; Na2···O7, 2.399(3) Å; Na2···O2, 2.424(3) Å; and Na2···O6, 2.451(3) Å) and have secondary contacts with one O atom and one N atom (Na1···O6, 2.843(3) Å; Na1···N2, 2.929(3) Å; Na2···O3, 2.806(3) Å; and Na2···N1, 2.907(3) Å), resulting in a highly distorted pentagonal bipyramid coordination. In both the cases, five TFSA$^-$ anions are involved in the coordination around Na$^+$, two of the five being working in a bidentate form.

The M$^+$ cation in M[TFSA] (M$^+$ = Li$^+$, Na$^+$, K$^+$, and Cs$^+$) have different interionic contacts with TFSA$^-$, depending on the size of M$^+$, which are shown in Fig. 4. Bond valence sum was calculated for M$^+$ in M[TFSA] to compare the coordination state of each site with that in others and to evaluate

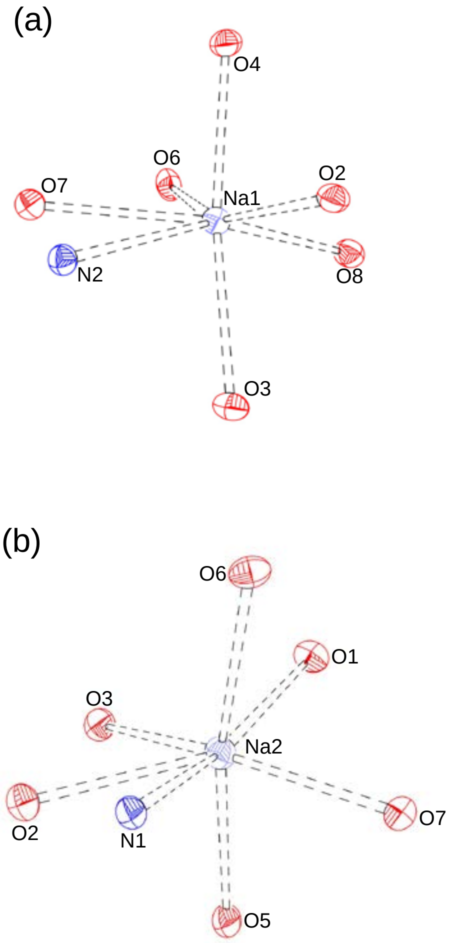

Fig. 3 Coordination environment around the two crystallographically independent Na^+ atoms in Na[TFSA].

the contribution of each contact to the coordination state. Bond valence (v) is given by the following eq. (1):

$$v = \exp[(R_0 - R) / B] \quad (1)$$

where R_0 (Å) = 1.466 for Li···O, 1.803 for Na···O, 1.93 for Na···N, 2.132 for K···O, 2.26 for K···N, 2.147 for Cs···O, and 2.53 for Cs···N, B = 0.37, and R (Å) is the observed contact distance [25, 26]. Bond valence sum is then obtained as the sum of v over the bond valences for all interactions of M^+

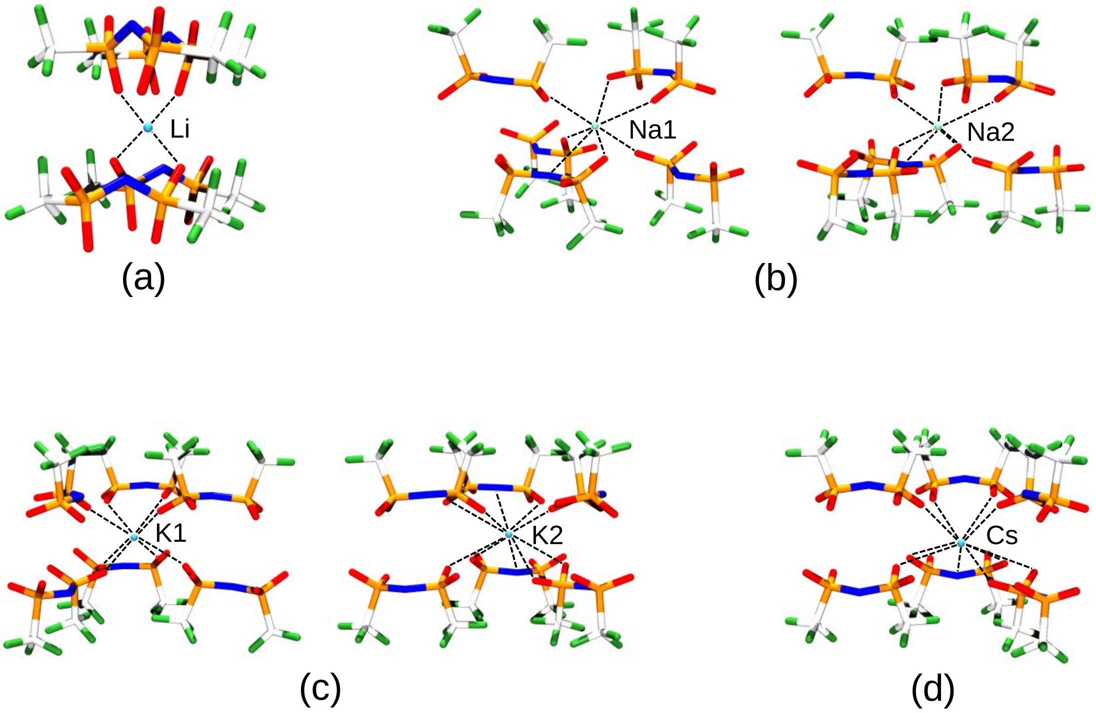

Fig. 4 Comparison of the intermolecular interactions of M^+ in M[TFSA] ((a) Li[TFSA] [5], (b) Na[TFSA], (c) K[TFSA] [3], and (d) Cs[TFSA] [3]).

to its neighboring atoms. Results of the bond valence sum calculations are summarized in Table 3.

Coordination number of M^+ in M[TFSA] increases with an increase in the size of M^+. The Li^+ cation has contacts with four O atoms of four different *trans*-$TFSA^-$ anions in a slightly distorted tetrahedral manner [5]. The bond valence sum of Li^+ in Li[TFSA] is 1.06 and is slightly larger than those in Li[TFSA]·H_2O where all of the six crystallographically independent Li^+ atoms are octahedrally coordinated to six O atoms (one or two O atoms from H_2O molecules and the others from *cis*-$TFSA^-$ anions) with the bond valence sums of 0.96, 0.97, 0.98, 0.98, 1.00, and 1.01; see Supplementary Contents for the calculation of bond valences in the case of Li[TFSA]·H_2O.

The bond valence sums of Na1 and Na2 in Na[TFSA] are similar to each other (1.17 and 1.15, respectively). These values are close to that in the previously known solvate Na[TFSA]·H_2O·CH_3OH (1.16) where Na^+ has contacts with six O atoms (four from $TFSA^-$ and two from H_2O [3]; see Supplementary Contents for the calculation of bond valences in the case of

Table 3 Contact distances (Å), the corresponding bond valences, and bond valence sum (BVS) for M$^+$ in M[TFSA] (M = Li$^+$, Na$^+$, K$^+$, and Cs$^+$)[a]

Compound	Contact atoms	Contact distance / Å	Bond valence
Li[TFSA][b]	Li···O	1.95	0.27
	Li···O	1.95	0.27
	Li···O	1.97	0.26
	Li···O	1.97	0.26
			BVS 1.06
Na[TFSA][c]	Na1···O	2.344	0.23
	Na1···O	2.346	0.23
	Na1···O	2.395	0.20
	Na1···O	2.411	0.19
	Na1···O	2.415	0.19
	Na1···O	2.843	0.06
	Na1···N	2.929	0.07
			BVS 1.17
	Na2···O	2.337	0.24
	Na2···O	2.385	0.21
	Na2···O	2.399	0.20
	Na2···O	2.424	0.19
	Na2···O	2.451	0.17
	Na2···O	2.806	0.07
	Na2···N	2.907	0.07
			BVS 1.15
K[TFSA][d]	K1···O	2.697	0.22
	K1···O	2.724	0.20
	K1···O	2.726	0.20
	K1···O	2.742	0.19
	K1···O	2.791	0.17
	K1···O	2.848	0.14
	K1···O	2.882	0.13
	K1···O	2.996	0.10
			BVS 1.35
	K2···O	2.800	0.16
	K2···O	2.873	0.13
	K2···O	2.895	0.13
	K2···O	2.959	0.11
	K2···O	3.113	0.07
	K2···O	3.114	0.07
	K2···O	3.204	0.06
	K2···O	3.343	0.04
	K2···N	3.405	0.05
	K2···N	3.413	0.04
			BVS 0.86
Cs[TFSA][d]	Cs···O	3.037	0.19
	Cs···O	3.091	0.16
	Cs···O	3.150	0.14
	Cs···O	3.177	0.13
	Cs···O	3.212	0.12
	Cs···O	3.242	0.11
	Cs···N	3.294	0.13
	Cs···O	3.328	0.09
	Cs···O	3.646	0.04
	Cs···O	3.706	0.03
			BVS 1.14

[a] Bond valence was calculated by eq. (1) where R_0 (Å) = 1.466 for Li···O, 1.803 for Na···O, 1.93 for Na···N, 2.132 for K···O, 2.26 for K···N, 2.147 for Cs···O, and 2.53 for Cs···N, B = 0.37, and R (Å) is the observed contact distance [25, 26] . [b] The crystallographic data are from Ref. [5]. [c] This study. [d] The crystallographic data are from Ref. [3].

$Na[TFSA]\cdot H_2O\cdot CH_3OH$. The ratio of a bond valence to the bond valence sum roughly gives a quantitative measure about contribution of the corresponding contact to the coordination state of the cation. Although the bond valences of the secondary contacts in Na[TFSA] are 0.06 for Na1···O6, 0.07 for Na1···N2, 0.07 for Na2···O3, and 0.07 for Na2···N1 and are certainly small compared to those of the primary contacts (0.21 in average), they are not negligible.

The crystallgraphically independent two K^+ cations in K[TFSA] have different coordination from each other [3]. One K^+ atom (K1 in Fig. 4 (c)) has contacts with eight O atoms of six $TFSA^-$ anions in a distorted square antiprism way, two of the six $TFSA^-$ anions being working in a bidentate form. The distribution of the contact distances around K1 is narrow ranging from 2.697 to 2.996 Å. The other K^+ atom (K2 in Fig. 4 (c)) is located in a totally different environment where eight O atoms and two N atoms are involved. The contact distances around K2 widely ranges from 2.800 to 3.413 Å and their average is longer than that around K1. Bond valence sum analysis gives quite unusual values for these two K^+ ions; the bond valence sum for K1 (1.35) is significantly larger than that for K2 (0.86). Even considering the errors of the present R_0 and B parameters, this difference can be regarded to be significant and strongly suggests the coordination state of the two K sites are quite different from each other.

The Cs[TFSA] structure contains only one crystallographically independent Cs^+ [3]. Seven O atoms and one N atom are in the range of primary contacts, whereas other two O atoms are in the range of secondary contacts. In total, six $TFSA^-$ anions are involved in the coordination around Cs^+, where three of them are monodentate, two of them are bidentate, and one of them are tridentate. In terms of coordination geometry, four contacts from the top and six contacts from the bottom in Fig. 4 (d) give a highly asymmetric coordination environment. This is reflected to the difference in the bond valences between the top and bottom; the four contacts from the top have short contact distances ranging from 3.037 to 3.177 Å with bond valences of 0.19, 0.16, 0.14, and 0.13 and the six contacts from the bottom do ranging from 3.212 to 3.706 Å with bond valences of 0.12, 0.11, 0.13, 0.09, 0.04, and 0.03. The sums of the bond valences for Cs^+ from the top and bottom are 0.62 and 0.52, suggesting Cs^+ is more strongly coordinated from the top side.

3. Conclusions

This study reported the crystal structure of Na[TFSA] and coordination environment of M^+ in the M[TFSA] salts (M = Li^+, Na^+, K^+, and Cs^+). The layered structure of Na[TFSA] is highly related to those observed in previously known alkali and alkali earth metal TFSA salts and their solvate forms. Coordination environment of M[TFSA] differs depending on the size of the cation. Bond valence sum calculations gave information about the difference and similarity in environment for each cation site; the environments of the two Na^+ sites in Na[TFSA] are similar to each other, whereas those of the two K^+ sites in K[TFSA] are quite different from each other. The Cs site in Cs[TFSA] has an asymmetric coordination state from the anion layers.

4. Experimental

4.1 General experimental procedure

Moisture-sensitive materials were handled in a drybox under a dry Ar atmosphere. Volatile materials were handled in a reaction line made of stainless steel (SS-316, 1/2-inch o.d.) and tetrafluoroethylene-perfluoroalkylvinylether copolymer (PFA) which were connected by stainless steel unions and valves with Kel-F tips. The line was connected to a rotary vacuum pump through a liquid nitrogen trap (~1 Pa). The pressure and vacuum of the line were monitored by Bourdon and Pirani gauges.

4.2 Reagents

Bis(trifluoromethylsulfonyl)imide, $HN(SO_2CF_3)_2$ (Morita Chemical Industries, purity > 99 %) and Na_2CO_3 (Wako Pure Chemical Industries, purity > 99.5 %), and ethanol (Wako Pure Chemical Industries, purity > 99.5 %) were used as supplied.

4.3 Synthesis of Na[TFSA]

The sodium salt, Na[TFSA], was synthesized by neutralization of $HN(SO_2CF_3)_2$ and Na_2CO_3 in ethanol [18, 20]. The starting materials, $HN(SO_2CF_3)_2$ (14.1 g, 50.1 mmol) and $Na_2[CO_3]$ (2.65 g, 25.0 mmol) were weighed in the drybox and $HN(SO_2CF_3)_2$ was dissolved in ethanol (100 mL) in the air. Sodium carbonate was slowly added into the solution, followed by agitation for one hour. The end point of neutralization was confirmed by measuring the pH of the solution. The solvent ethanol was roughly removed by a rotary evaporator for a few hours. The obtained white powder was transferred into a glass vessel and dried under vacuum for three days at 423 K. Raman (frequency/cm^{-1} (relative intensity)): 1335(6), 1320(14), 1238(39), 1225(6), 1218(4), 1210(4), 1199(2), 1153(24), 1135(5), 803(3), 775(2), 747(100), 659(15), 607(3), 591(3), 576(7), 565(7), 556(10), 539(3), 515(3), 436(7), 411(14), 357(13), 335(54), 315(16), 287(21), 298(13), 236(3), 214(1), 181(3), 133(14), and 92(9) ($TFSA^-$). Infrared (frequency/cm^{-1} (relative intensity, vw: very weak, w: weak, m: middle, s: strong)): 407(w), 420(vw), 436(w), 455(vw), 471(vw), 513(s), 532(vw), 554(vw), 573(s), 592(s), 642(w), 652(w), 743(m), 772(vw), 797(m), 1049(s), 1136(s), 1200(s), 1229(vw), 1242(vw), 1315(m), 1337(m), and 1366(m) ($TFSA^-$) (see Supplementary Contents for the Raman and infrared specra).

4.4 Spectroscopic analysis

The infrared spectrum was obtained by an FTIR spectrometer, FTS155 (Bio−RAD Laboratories). The solid sample finely ground in a mortar was sandwiched between a pair of AgCl windows in an air-tight cell. The gaseous samples were introduced into a stainless steel air-tight cell with a pair of AgCl windows. The Raman spectrum was recorded (FTS-175C, Bio-Rad Laboratories) at room temperature using the 1064 nm line of a Nd:YAG laser as the excitation line. The sample for Raman spectroscopy was loaded in an aluminum pan, which was sealed in an airtight unit with a glass window.

4.5 Crystal growth and X-ray diffraction analysis

Crystals of Na[TFSA] were grown by slow cooling of the sample from its molten state in a quartz capillary (0.5 mm in o.d.). The single crystal used for data collection was a colorless transparent chunk measuring 0.15×0.15×0.15 mm^3. The diffraction data was measured by a diffractometer (R−axis Rapid II, Rigaku[27] controlled by the program RAPID AUTO 2.40[28]) using MoKα radiation (λ= 0.710747 Å). Data collection was performed at 100 K and consisted of 12 ω scans (130−190°, 5° per frame) at the fixed φ (0°) and χ(45°) angles and 32 ω scans (0−160°, 5° per frame) at fixed φ (180°) and χ (45°) angles. The exposure time was 1200 s deg^{-1}. Integration, scaling and absorption corrections were performed using RAPID AUTO 2.40. The structure was solved using SIR−92[29] and refined by SHELXL−97[30] linked to Win−GX[31]. Anisotropic displacement factors were introduced for all atoms.

Crystallographic data (excluding structure factors) has been deposited with the Cambridge Crystallographic Data Centre as supplementary publication no. CCDC 1007351. Copies of the data can be obtained, free of charge, on application to CCDC, 12 Union Road, Cambridge CB2 1EZ, UK (fax: +44 1223 336033 or deposit@ccdc.cam.ac.uk).

Appendix A. Supplementary data

Supplementary data associated with this article can be found, in the online version, at doi:10.1016/j.jfluchem.xxx.

Figure captions

Fig. 1 ORTEP diagram of the asymmetric unit of Na[TFSA]. Thermal ellipsoids are shown at the 50% probability level.

Fig. 2 Packing diagram of Na[TFSA] along the *b* axis. Thermal ellipsoids are shown at the 50% probability level.

Fig. 3 Coordination environment around the two crystallographically independent Na^+ atoms in Na[TFSA].

Fig. 4 Comparison of the intermolecular interactions of M^+ in M[TFSA] ((a) Li[TFSA] [5], (b) Na[TFSA], (c) K[TFSA] [3], and (d) Cs[TFSA] [3]).

References

[1] J. Foropoulos, D.D. Desmarteau, J. Am. Chem. Soc., 104 (1982) 4260-4261.

[2] J. Foropoulos, D.D. Desmarteau, J. Fluorine Chem., 21 (1982) 9-9.

[3] L.X. Xue, C.W. Padgett, D.D. DesMarteau, W.T. Pennington, Solid State Sci., 4 (2002) 1535-1545.

[4] L.X. Xue, D.D. DesMarteau, W.T. Pennington, Solid State Sci., 7 (2005) 311-318.

[5] J.L. Nowinski, P. Lightfoot, P.G. Bruce, J. Mater. Chem., 4 (1994) 1579-1580.

[6] Z. Zak, A. Ruzicka, C. Michot, Z. Kristallogr., 213 (1998) 217-222.

[7] M.J. Earle, U. Hakala, B.J. McAuley, M. Nieuwenhuyzen, A. Ramani, K.R. Seddon, Chem. Commun., (2004) 1368-1369.

[8] A. Haas, C. Klare, P. Betz, J. Bruckmann, C. Kruger, Y.H. Tsay, F. Aubke, Inorg. Chem., 35 (1996) 1918-1925.

[9] J.J. Golding, D.R. Macfarlane, L. Spiccia, M. Forsyth, B.W. Skelton, A.H. White, Chem. Commun., (1998) 1593-1594.

[10] C.M. Forsyth, D.R. MacFarlane, J.J. Golding, J. Huang, J. Sun, M. Forsyth, Chem. Mater., 14 (2002) 2103-2108.

[11] P. Bonhote, A.P. Dias, N. Papageorgiou, K. Kalyanasundaram, M. Gratzel, Inorg. Chem., 35 (1996) 1168-1178.

[12] D.R. MacFarlane, P. Meakin, J. Sun, N. Amini, M. Forsyth, J. Phys. Chem. B, 103 (1999)

4164-4170.

[13] J.D. Holbrey, W.M. Reichert, R.D. Rogers, Dalton Trans., (2004) 2267-2271.

[14] F.B. Dias, L. Plomp, J.B.J. Veldhuis, J. Power Sources, 88 (2000) 169-191.

[15] H. Tokuda, K. Ishii, M.A.B.H. Susan, S. Tsuzuki, K. Hayamizu, M. Watanabe, J. Phys. Chem. B, 110 (2006) 2833-2839.

[16] K. Tsunashima, M. Sugiya, Electrochem. Commun., 9 (2007) 2353-2358.

[17] A. Noda, K. Hayamizu, M. Watanabe, J. Phys. Chem. B, 105 (2001) 4603–4610.

[18] R. Hagiwara, K. Tamaki, K. Kubota, T. Goto, T. Nohira, J. Chem. Eng. Data, 53 (2008) 355-358.

[19] A. Watarai, K. Kubota, M. Yamagata, T. Goto, T. Nohira, R. Hagiwara, K. Ui, N. Kumagai, J. Power Sources, 183 (2008) 724-729.

[20] T. Nohira, T. Ishibashi, R. Hagiwara, J. Power Sources, 205 (2012) 506-509.

[21] D.R. MacFarlane, J.H. Huang, M. Forsyth, Nature, 402 (1999) 792-794.

[22] J.M. Pringle, P.C. Howlett, D.R. MacFarlane, M. Forsyth, J. Mater. Chem., 20 (2010) 2056-2062.

[23] K. Fujii, T. Fujimori, T. Takamuku, R. Kanzaki, Y. Umebayashi, S.I. Ishiguro, J. Phys. Chem. B, 110 (2006) 8179-8183.

[24] J.N.C. Lopes, A.A.H. Padua, J. Phys. Chem. B, 108 (2004) 16893-16898.

[25] I.D. Brown, D. Altermatt, Acta Crystallogr. B, 41 (1985) 244-247.

[26] N.E. Brese, M. Okeeffe, Acta Crystallogr. B, 47 (1991) 192-197.

[27] RAPID XRD, version 2.3.3, Rigaku Corporation Tokyo, Japan, 1999-2004.

[28] RAPID AUTO, version 2.40, Rigaku Corporation, Tokyo, Japan, 2006.

[29] A. Altomare, G. Cascarano, C. Giacovazzo, A. Guagliardi, J. Appl. Crystallogr., 26 (1993) 343-350.

[30] G.M. Sheldrick, Acta. Crystallogr. A, 64 (2008) 112-122.

[31] L.J. Farrugia, J. Appl. Crystallogr., 32 (1999) 837-838.